Injection Molding and Injection Compression Molding of Thin-Walled Light-Guided Plates with V-Grooved Microfeatures

Ming-Shyan Huang, Chin-Feng Chung

Department of Mechanical and Automation Engineering and Graduate Institute of Industrial Design, National Kaohsiung First University of Science and Technology, 2 Jhuoyue Road, Nanzih, Kaohsiung City 811, Taiwan, Republic of China

Received 16 July 2010; accepted 13 October 2010
DOI 10.1002/app.33603
Published online 28 February 2011 in Wiley Online Library (wileyonlinelibrary.com).

ABSTRACT: In this study, we investigated the feasibility of injection molding (IM) and injection compression molding (ICM) for fabricating 3.5-in. light-guided plates (LGPs). The LGP was 0.4 mm thick with v-grooved microfeatures (10 μm wide and 5 μm deep). A mold was designed to fabricate LGPs by IM and ICM. Micromachining was used to make the mold insert. The Taguchi method and parametric analysis were applied to examine the effects of the process parameters on the molding quality. The following parameters were considered: barrel temperature, mold temperature, packing pressure, and packing time. Mold temperature in this investigation was in the conventional range. Increasing the barrel temperature and mold temperature generally improved the polymer melt fill in the cavities with microdimensions. The experimental results for the replication of microfeatures by IM and ICM are presented and compared. The height of the v-grooved microfeatures replicated by ICM was more accurate than those replicated by IM. Additionally, the flatness of the fabricated LGPs showed that ICM was better than IM for thin-walled molding. © 2011 Wiley Periodicals, Inc. J Appl Polym Sci 121: 1151–1159, 2011

Key words: injection compression molding; injection molding; light-guided plates; microfeatures

INTRODUCTION

A light-guided plate (LGP), a key component of backlight modules in liquid crystal displays, directs light propagation to improve luminance and uniformity. The microstructures of LGPs are key control factors; thus, the replication effect determines the optical performance of LGPs. For instance, Lin et al.[1] reported that the luminance of LGPs showed a strong correlation with the depth of the melt filling of the v-grooves. Injection molding (IM) is one of the most common processes for manufacturing microfeatured parts.[2–7] A significant advantage of IM is that it can produce complex geometries during one automated process. The IM process generally has three phases: the filling, packing, and cooling phases. After the cavity stabilizes, the product is ejected from the mold.

Despite its many advantages, IM has some inherent problems in molding microfeatures.[8–10] The primary difficulty is that molten polymers in a tiny cavity instantaneously freeze once they touch the relatively cooler cavity wall. This problem worsens when microfeatures with high aspect ratios are molded. The best replication results were achieved when the melt temperature and mold temperature exceeded normal values. Yoshii et al.[11] demonstrated that increasing mold temperature only enhanced the replication effect of the microgrooves. To achieve a high mold temperature during the filling phase and then a decrease of mold temperature to below the heat deflection temperature during the packing and cooling phase without increasing the cycle time, the rapid thermal cycling of injection molds can be used.[12] Another approach is to use an ultrahigh injection speed to provide a better melt filling of microfeatures due to the high viscous heating and cavity pressure during transcription molding at ultrahigh injection speeds.[13] Chen et al.[14] determined that increasing the plastic temperature, mold temperature, injection speed, and packing pressure enhanced the luminance performance of an LGP. However, residual stress exists in LGPs, and the uniformity of the microfeatures remains a problem with IM. Injection compression molding (ICM) was developed to solve these problems.

Notably, ICM introduces a compression action into the filling process. With a reliance on pressure

Correspondence to: M.-S. Huang (mshuang@nkfust.edu.tw).
Contract grant sponsor: Ministry of Economics Affairs of the Republic of China; contract grant number: 98-EC-17-A-07-S1-108.

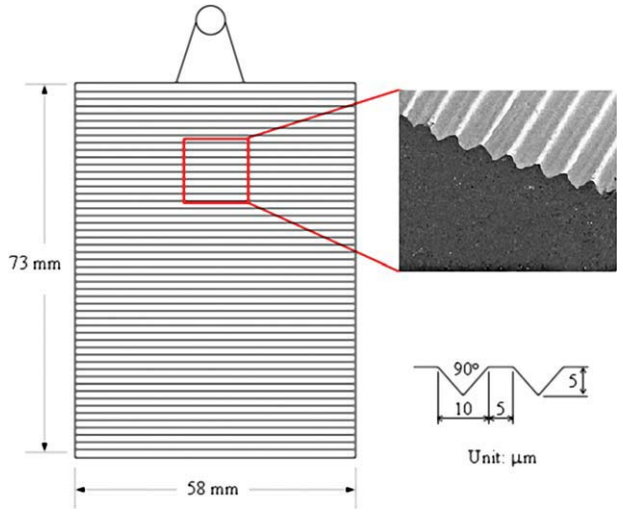

Figure 1 LGP (3.5-in.) with v-grooved microfeatures. [Color figure can be viewed in the online issue, which is available at wileyonlinelibrary.com.]

transmitted from the glue sprue, pressure is also imposed by a compression action from the mold wall. This process has many advantages, including even packing, less molding pressure, less residual stress, less molecular orientation, less uneven shrinkage, less density variation, less warpage, and better dimensional accuracy than found with the IM process. On the basis of these advantages, ICM is typically used to fabricate parts requiring a high accuracy and no residual stress, such as LPGs. For instance, Yang and Ke[15] used ICM to fabricate round plates and found that less molecular orientation and internal stress remained than when IM was used. Finished product quality can, thus, be improved, and thickness differences can be eliminated. Chen et al.[16] determined that the cavity pressure variation with molding an optical disc by ICM was lower than that by IM. Wu and Chen[17] compared applications of IM and ICM processes to produce diffraction gratings; the diffraction pattern indicated that ICM was a better process than IM for replicating a diffraction grating. Tseng and Liao[18] applied ICM to effectively eliminate the residual stress of diffraction optical elements; the experimental results revealed that compression speed dominated the cavity pressure distribution and became the most important factor affecting the final optical properties. Wu and Su,[19] who used ICM to reduce the shrinkage of LGPs, found that the mold and barrel temperatures and injection speed were the key parameters for enhancing the accuracy of the optical components and eliminating shrinkage. Liu and Lin,[20] who applied ICM to wedge plates, concluded that an appropriate compression pressure and timing could reduce birefringence. Shen et al.[21] applied ICM to mold 2-in. LGPs. Their investigation demonstrated that the replication effects of microstructures were improved with increasing plastic temperature and were dependent on the proper compression distance and speed.

Although many studies have applied ICM for microinjection molding, the geometrical dimensions of microstructures are limited to 10s of micrometers. Particularly, studies using ICM for thin-walled molding have been rare. In this study, we compared the performances of IM and ICM in the fabrication of LGPs, which were 0.4 mm thick and had 5–10-μm microstructures, to achieve high luminance and optical quality. In this study, we also investigated the effects of ICM on thin-walled microinjection molding, which requires a high replication rate and a low degree of warpage; major factors, such as the compression pressure, distance, and speed, were also examined.

EXPERIMENTAL

Material, part geometry, mold design, and molding machine

Polymethyl methacrylate (Kuraray GH-1000S, made in Japan) was used in this experiment and had a glass-transition temperature of 104°C. The molded part was a 3.5-in. flat LGP that was 73 mm long, 58

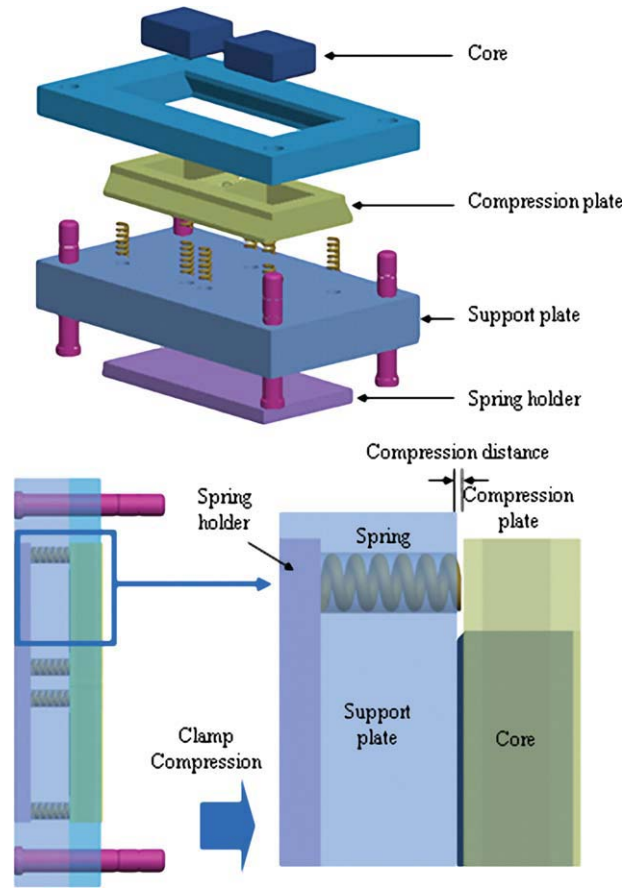

Figure 2 Structure of an injection compression mold. [Color figure can be viewed in the online issue, which is available at wileyonlinelibrary.com.]

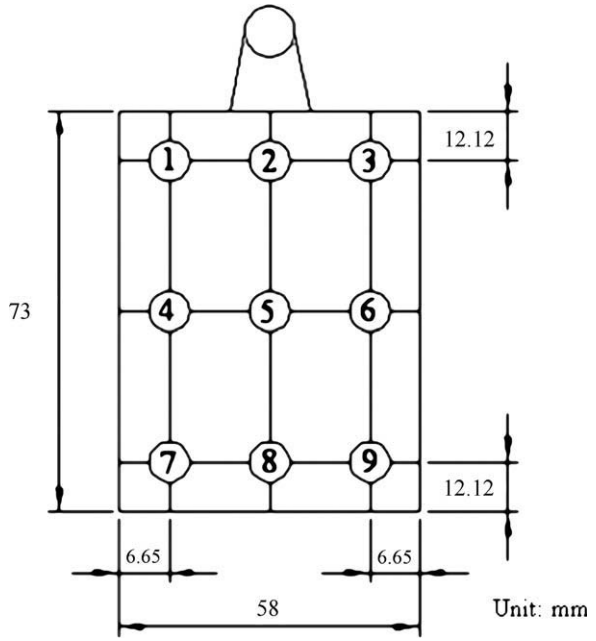

Figure 3 Measured locations of the microfeatures on a 3.5-in. LGP.

mm wide, and 0.4 mm thick (Fig. 1). The LGP had uniform micrometer-sized features of v-grooves (10 μm wide, 5 μm deep, and 15 μm in pitch, with a vertex angle of 90°). This single cavity mold was designed with a fan-shaped gate that was 40 mm wide and 0.4 mm thick. The IM and ICM trials were conducted with a mold base that complied with the requirement of modularity for using different mold inserts. Figure 2 shows the structure of the mold base used in both IM and ICM. In the moving half-mold, a compression plate was mounted with four support springs and touched the fixed half-mold, whereas the mold base was closed to align both mold halves. We controlled the *compression distance*, defined as the distance between the support plate and the compression plate, by controlling the position of the moving platen on the clamping unit. In this position, the mold was not closed completely, and the LGP could be molded with both IM and ICM. The mold inserts of the manufactured injection compression mold used in this investigation were made of beryllium copper machined into v-grooved microstructures.

TABLE I
Specifications of the Taylor Hobson Surface Profiler for Measuring the Microfeatures on LGP Mold Inserts and Molded Parts

Specification	Taylor Hobson
Model	Talysurf Laser 635
Scanning distance	0.5 mm
Scanning speed	0.1 mm/s
Probe radius	2.1 μm
Probe angle	40.2°

TABLE II
Depth of the Microfeatures of the LGP Mold Inserts

	Mold insert A (μm)		Mold insert B (μm)	
Position	Original	After compensation	Original	After compensation
p1	5.50	6.36	5.51	6.35
p2	5.49	6.34	5.51	6.34
p3	5.47	6.34	5.52	6.34
p4	5.49	6.36	5.48	6.34
p5	5.50	6.35	5.49	6.32
p6	5.51	6.35	5.47	6.30
p7	5.50	6.32	5.48	6.33
p8	5.53	6.37	5.49	6.32
p9	5.52	6.37	5.47	6.30
Average	5.50	6.35	5.54	6.33
Standard deviation	0.02	0.02	0.02	0.02

The molding operations were conducted with a high-speed, closed-loop hybrid IM machine (Fu Chun Shin AF-100, made in Taiwan). This machine had a clamping force of up to 100 tons. The screw diameter was 28 mm, and the maximum injection volume was 92 cm^3. This machine could be used during both ICM and IM. Under each set of process conditions, 10 runs were completed to ensure that the process was stable before the samples were fabricated. If no significant variation existed during these first 10 runs, molded parts from the next 2 runs were obtained as samples for product characterization.

Quality measurement

Two LGPs were sampled under each molding condition. Nine sampling positions on each sample were chosen for measuring the microgrooves (Fig. 3). After the samples were cooled for 24 h, LGP microfeatures were measured with a probe-touching surface profiler (Taylor Hobson surface profiler, made in US). This device is commonly used to measure microscale structures. This nondestructive detector is applicable for measuring samples characterized by transparency and conductivity, such as the geometry of optical injection-molded parts.[22] Table I lists the specifications of the Taylor Hobson surface profiler used in this study to measure the microfeatures of the LGP

TABLE III
Control Factors and Levels in the Taguchi Experiments for IM and ICM

	Level		
Control factor	1	2	3
A: Mold temperature (°C)	75	85	95
B: Melt temperature (°C)	260	270	280
C: Packing pressure (MPa)	50	60	70
D: Packing time (s)	1	2	3

TABLE IV
L_9 Orthogonal Array and Experimental Results for IM

Experiment	A	B	C	D	Height (μm) Average	Standard deviation	S/N	Replication rate (%)
1	1	1	1	1	5.29	0.45	14.47	83.4
2	1	2	2	2	5.41	0.43	14.66	85.3
3	1	3	3	3	5.56	0.39	14.93	87.7
4	2	1	2	3	5.53	0.41	12.85	87.2
5	2	2	3	1	5.62	0.29	14.99	88.6
6	2	3	1	2	5.75	0.28	15.19	90.7
7	3	1	3	2	5.84	0.12	14.32	92.1
8	3	2	1	3	5.88	0.15	15.41	92.7
9	3	3	2	1	5.95	0.11	15.49	93.9

mold inserts and molded parts. Table II lists the depths of the LGP microstructures on the two cavities before and after the compensation was measured. The data of the 9-point measuring positions (Fig. 3) revealed that the machining of the v-grooved microstructures was very accurate, and their depth was 6.34 ± 0.01 μm.

TAGUCHI PARAMETER DESIGN

The effects of the process parameters on the replication of the microfeatures of an LGP by IM and ICM were analyzed and compared. The Taguchi method was applied in this study. The signal-to-noise (S/N) ratio was used to measure deviation in quality from a desired value. The S/N ratio, instead of an average value, was also used to convert the experimental data into a value for evaluating the quality characteristics in optimum parameter analysis. The S/N ratio (dB) could be defined as follows:

$$S/N = -10 \log \text{MSD} \tag{1}$$

where MSD is the mean-squared deviation for output characteristics. The S/N ratio characteristics could be divided into three types—nominal is better, smaller is better, and larger is better—when the quality characteristics are continuous for engineering analysis. Because the study objectives were to identify the optimum settings that minimized replication errors in terms of the height of the LGP microfeatures, the smaller-is-better S/N ratio quality characteristic was used. MSD for the smaller-the-better quality characteristic could be expressed as follows:[22]

$$\text{MSD} = \frac{1}{mn} \sum_{j=1}^{m} \sum_{i=1}^{n} \Delta Y_{ij}^2 \tag{2}$$

where ΔY_{ij} is the difference between the measured value and target value for the ith sample and the jth measurement point, m is the total number of samples, and n is the total number of measurement points in one sample. Because the negative logarithm is a monotone decreasing function, S/N should have been maximized. Thus, S/N was calculated with eqs. (1) and (2). The error in the replicated height on the LGP under process parameters of mold temperature, melt temperature, packing pressure, and packing time were analyzed with the L_9 orthogonal array of the Taguchi method and their S/N ratios.

TABLE V
L_9 Orthogonal Array and Experimental Results for ICM

Experiment	A	B	C	D	Height (μm) Average	Standard deviation	S/N	Replication rate (%)
1	1	1	1	1	4.01	0.59	11.77	63.3
2	1	2	2	2	4.34	0.42	12.64	68.5
3	1	3	3	3	4.66	0.30	13.31	73.5
4	2	1	2	3	4.58	0.60	12.95	72.3
5	2	2	3	1	5.64	0.21	15.00	88.9
6	2	3	1	2	5.75	0.29	15.16	90.8
7	3	1	3	2	5.51	0.12	14.82	87.0
8	3	2	1	3	5.93	0.08	15.46	93.6
9	3	3	2	1	6.02	0.11	15.59	94.9

TABLE VI
ANOVA Results

SV	DOF	Var.	*F*	PSS	CP
IM					
A	2	0.787	83.45	0.787	81.66
B	2	0.156	13.51	0.156	14.37
C	2	0.011			
D	2	0.013			
Pooled error	0	0.020		0.020	2.97
Total	8	0.967			100.00
ICM					
A	2	11.483	55.71	11.48	69.04
B	2	3.776	16.97	3.38	21.04
C	2	0.654			
D	2	0.142			
Pooled error	0	0.80		0.80	9.92
Total	8	16.05			100.00

SV: source of variation; DOF: degrees of freedom; Var.: Variance; PSS: pure of sum squares; CP: contribution percentage.

The experiments were executed according to the L_9 orthogonal array for IM and ICM. Table III lists the control factors and levels in the Taguchi experiments. According to the short-shot experiment and the specification limits of the IM machine that we used, the following ranges of control factors were selected: mold temperature (A) = 75–95°C, melt temperature (B) = 260–280°C, packing pressure (C) = 50–70 MPa, and packing time (D) = 1–3 s. Each of

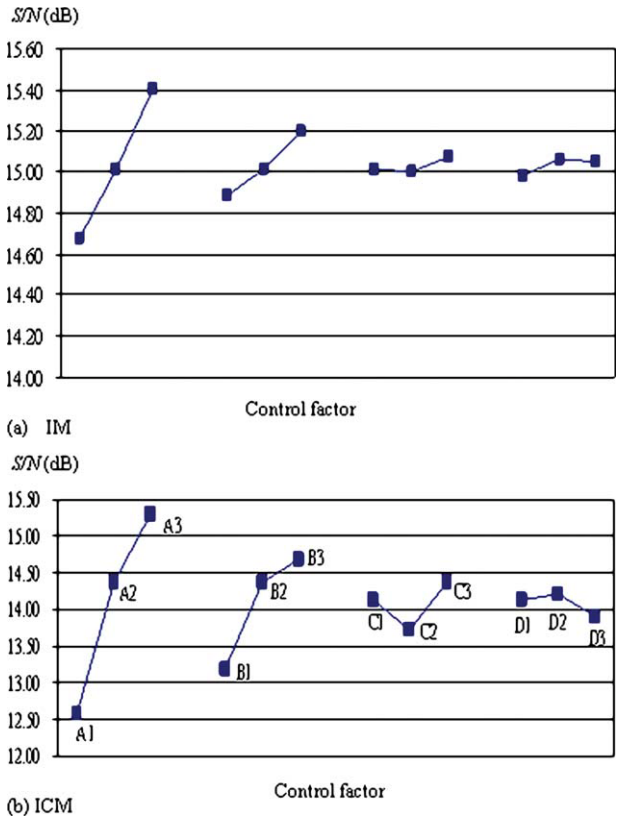

Figure 4 *S/N* response diagram. [Color figure can be viewed in the online issue, which is available at wileyonlinelibrary.com.]

TABLE VII
Confirmation Test of the 3.5-in. LGP Microinjection-Molded by IM and ICM

Position	Sample 1	Sample 2	Sample 3	Sample 4	Average
IM					
p1	5.64	5.68	5.78	5.72	5.71
p2	5.64	5.64	5.64	5.62	5.64
p3	6.08	5.82	5.87	5.91	5.92
p4	6.57	6.38	6.45	5.88	6.32
p5	5.73	5.71	5.77	6.12	5.83
p6	6.05	6.05	6.11	6.18	6.10
p7	5.79	5.89	5.88	5.87	5.86
p8	5.85	6.02	5.96	5.97	5.95
p9	6.22	6.15	6.21	6.15	6.18
Average	5.95	5.93	5.96	5.94	5.95
Standard deviation	0.31	0.25	0.25	0.19	0.22
S/N	15.46	15.44	15.49	15.46	15.46
Replication rate (%)	93.6	93.2	93.7	93.4	93.5
ICM					
p1	6.13	6.11	6.08	6.17	6.12
p2	6.09	6.09	6.07	6.14	6.10
p3	6.11	6.14	6.11	6.14	6.13
p4	6.18	6.12	6.12	6.15	6.14
p5	6.01	6.17	6.09	6.06	6.08
p6	6.08	6.08	6.09	6.12	6.09
p7	6.03	6.09	6.14	6.16	6.11
p8	6.13	6.12	6.17	6.15	6.14
p9	6.16	6.03	6.16	6.07	6.11
Average	6.10	6.11	6.11	6.13	6.11
Standard deviation	0.06	0.04	0.04	0.04	0.02
S/N	15.71	15.71	15.73	15.75	15.73
Replication rate (%)	96.2	96.3	96.3	96.6	96.4

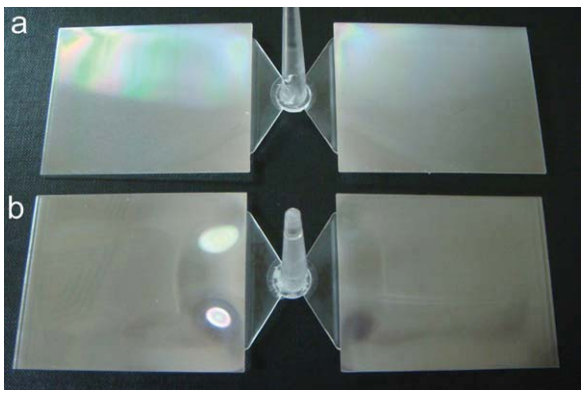

Figure 5 LGP (3.5-in.) microinjection-molded parts: (a) IM part (lower) and (b) ICM part (upper). [Color figure can be viewed in the online issue, which is available at wileyonlinelibrary.com.]

the four molding factors is designed with three levels because of possible nonlinear factor effects. Tables IV and V list the IM and ICM experimental results from nine runs based on the orthogonal array L_9, consisting of four experimental factors; each factor had three levels.

IM AND ICM QUALITY RESULTS

Tables IV and V present the experimental results for the replication of the v-groove height by IM and ICM, respectively. The aim of this study was to identify the optimal settings that maximized the replication rate of the height of the microfeatures.

Effects of the molding factors on the replication accuracy

Table VI lists the analysis of variance (ANOVA) results from analysis of the significance of the process parameters to height replication by IM and ICM. The analysis of the percentage contribution of variance suggested that control factor A was the most influential factor with a contribution of 81.66% for IM and 69.04% for ICM; the next most influential was control factor B, with a contribution of 14.37% for IM and 21.04% for ICM.

Optimum set of the molding parameters

Figure 4(a,b) shows S/N for height replication by IM and ICM, respectively. These figures present the effects of the process factors on height replication. By using the optimal levels of the parameters (Fig. 4), we determined the maximum height replication using eq. (2) for fabricating LGPs with polymethyl methacrylate. As mold temperature and melt temperature had very strong effects on the height replication rate, they were used to calculate the maximum S/N ratio for height replication.

The maximum S/N ratio for height replication by IM and ICM was derived as

$$\text{Maximum } S/N \text{ ratio} = T + (A3 - T) + (B3 - T) \quad (3)$$

where T is the average S/N of response for height replication and $A3$ and $B3$ are the third-level S/N values of control factors A and B, respectively.

For IM, the maximum S/N ratio for height replication was 15.57 dB, and the range of the S/N ratio at the 95% confidence level was 15.32–15.82 dB. For ICM, the maximum S/N ratio for height replication was 15.90 dB, and the range of the S/N ratio at the 95% confidence level was 14.94–16.86 dB.

Verification test

In this study, a verification test was conducted with the optimum levels of the process parameters, such as $A3B3C3D2$, for maximal replication rate in height from the IM and ICM optimization processes. On

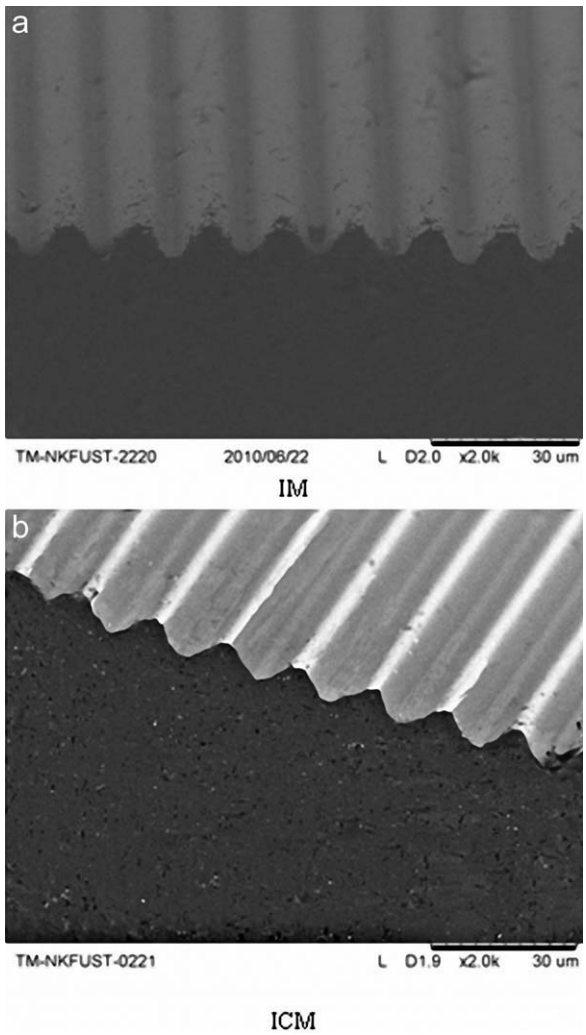

Figure 6 SEM micrographs of the v-grooves on molded parts by IM (upper) and ICM (lower) at the p7 location.

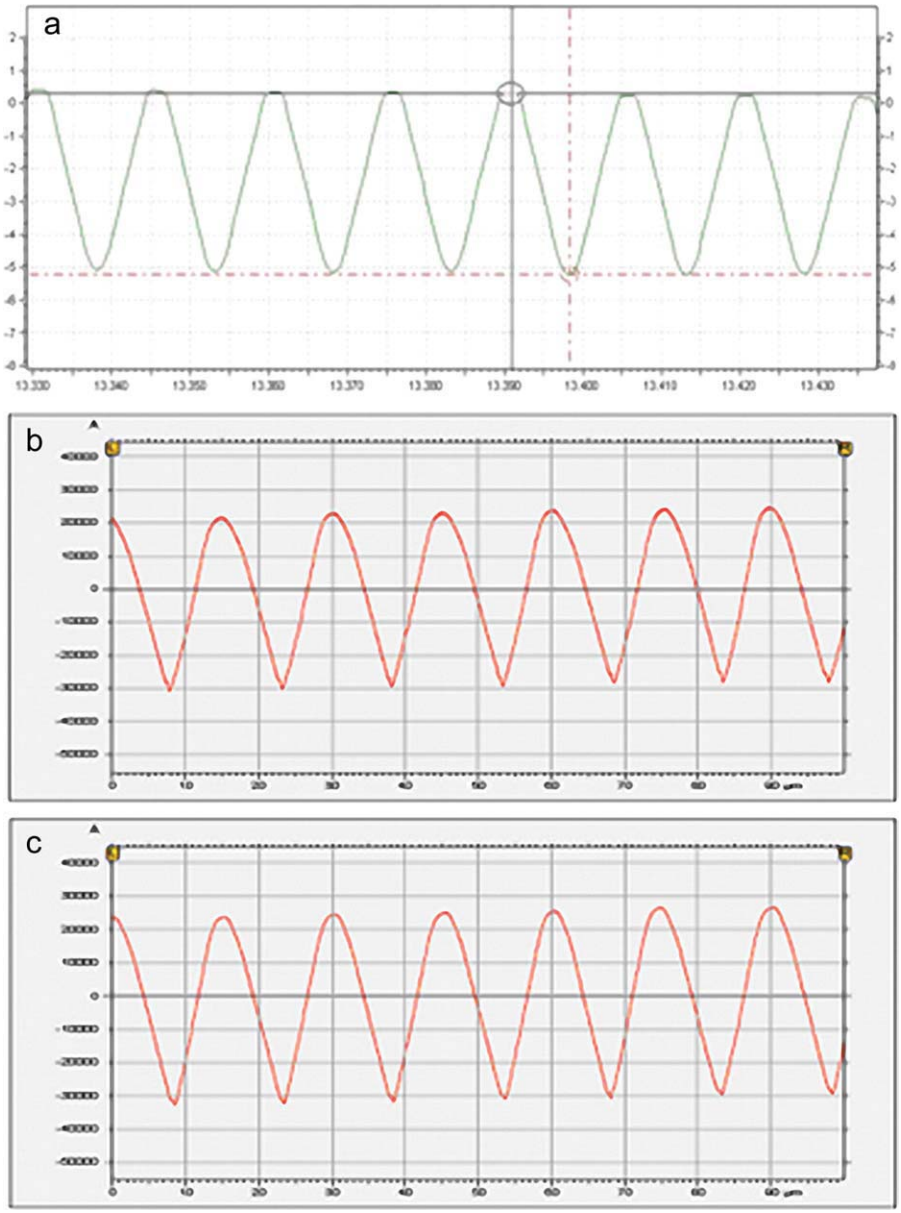

Figure 7 Cross-sectional surface profiles of the 3.5-in. LGP microinjection-molded parts at the p5 location: (a) mold insert (upper), (b) IM part (middle), and (c) ICM part (lower). [Color figure can be viewed in the online issue, which is available at wileyonlinelibrary.com.]

the basis of the optimum levels of the process parameters, the height replication values were obtained. Table VII shows the experimental results by IM and ICM. On the basis of measurements of the four ICM samples fabricated under the optimal settings, the performance in replicating the v-grooved microstructure height was higher (96.4% replication rate) than that of the IM samples (93.5% replication rate).

Comparison between the IM and ICM parts

With the optimum set of process conditions, parts were fabricated by IM and ICM. These two processes were examined by comparison of the qualities of the IM and ICM parts. The ICM part was flatter than the IM part (Fig. 5).

TABLE VIII
Control Factors and Levels of the Taguchi Experiments for ICM (Experiment 2)

Control factor	Level 1	Level 2	Level 3
A: Injection speed (mm/s)	200	350	525
B: Screw position (mm)	21	23	25
C: Compression speed (%)	50	75	100
D: Compression distance (mm)	0.5	0.9	1.3

TABLE IX
L_9 Orthogonal Array and Experimental Results for ICM (Experiment 2)

					Height (μm)			
Experiment	*A*	*B*	*C*	*D*	Average	Standard deviation	*S/N*	Replication rate (%)
1	1	1	1	1	5.56	0.28	14.88	87.7
2	1	2	2	2	5.54	0.33	14.83	87.4
3	1	3	3	3	5.55	0.22	14.86	87.5
4	2	1	2	3	5.30	0.38	14.42	83.5
5	2	2	3	1	5.84	0.27	15.31	92.1
6	2	3	1	2	5.89	0.26	15.39	92.9
7	3	1	3	2	6.01	0.20	15.58	94.8
8	3	2	1	3	6.00	0.23	15.56	94.7
9	3	3	2	1	5.46	0.46	14.65	86.1

From the experimental results shown in Table VII, we determined that the uniformity of the microfeatures at different locations of the molded parts differed. For parts fabricated by IM, the degree of replication at the p2 and p5 positions, that is, at the center of the part, was relatively low. Additionally, the degree of replication at the p1, p2, and p3 positions (near the gate) was significantly lower than that at p7, p8, and p9 (far from the gate). Through ICM, the uniformity of the microfeatures at different locations of the parts was significantly improved (Table VII).

The molded LGPs were also examined by scanning electron microscopy (SEM). Figure 6(a,b) shows the SEM micrographs of the v-grooves on the IM and ICM parts at the p7 location, respectively. Figure 7(a–c) show the cross-sectional surface profiles at the p5 location on the mold insert, the IM part, and the ICM part, respectively. We determined that the micromolding replication effect was stronger for the ICM parts than for the IM parts.

EFFECTS OF THE COMPRESSION PRESSURE, COMPRESS DISTANCE, AND COMPRESSION SPEED ON THE ICM PARTS

On the basis of the optimal parameter settings, in this study, we investigated the effects of the compression pressure, compression distance, and compression speed on the mold quality by ICM. Experiments were executed with the L_9 orthogonal array. Table VIII lists the control factors and levels in the Taguchi experiments. According to the short-shot experiment and specification limits of the IM machine that we used, the following ranges of control factors were selected: injection speed (*A*), 200–525 mm/s, screw position (*B*) = 21–25 mm, compression speed (*C*) = 50–100%, and compression distance (*D*) = 0.5–1.5 mm. Each of these four molding factors had three levels to eliminate possible nonlinear factor effects. Table IX lists the experimental results of nine runs based on the orthogonal array L_9, consisting of four experimental factors with three levels for each factor.

Table X lists the ANOVA results of the evaluation of the effects of the process parameters on the height replication by ICM. The analysis of the percentage contribution of variance indicated that control factor *C* (compression speed) was the most influential factor, with a contribution of 56.88% for ICM, followed by control factor *A* (injection speed), with a contribution of 18.14%; the third factor was *D* (compression distance), with a contribution of 14.47%, and the fourth factor was *B* (screw position), with a contribution of 10.1%. Figure 8 is constructed on the basis of the *S/N* ratio response for the height replication by ICM. This figure illustrates the effects of the process factors on the height replication. The

TABLE X
ANOVA Results for ICM (Experiment 2)

SV	DOF	Var.	*F*	PSS	CP
A	2	0.252	—	0.252	18.14
B	2	0.146	—	0.146	10.51
C	2	0.788	—	0.788	56.88
D	2	0.201	—	0.201	14.47
Pooled error	0				
Total	8				100.00

SV: source of variation; DOF: degrees of freedom; Var.: Variance; PSS: pure of sum squares; CP: contribution percentage.

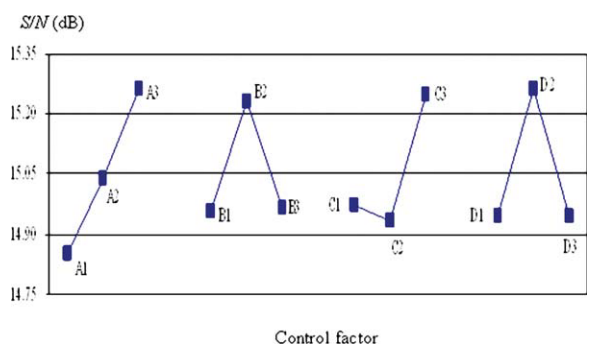

Figure 8 *S/N* response diagram for ICM (experiment 2). [Color figure can be viewed in the online issue, which is

optimum process parameters were *A3B2C3D2* for maximum height replication from the ICM optimization process. On the basis of the optimum levels of the process parameters, a confirmation test was again performed in this study. The experimental result shows that ICM reached a high precision of 96.8% (average height replication rate). This was because the compression process provided a higher and more uniform pressure distribution inside the cavity, and thus, it helped to replicate the microfeatures.[18] Additionally, the importance of the compression speed and compression distance was the same as that determined by Shen et al.[21] Notably, the injection speed was an important factor in the process of thin-walled ICM. This novel finding indicated that rapid cooling of thin-walled parts may affect ICM quality. Thus, a high injection speed is useful to ensure that parts are molded under compressible conditions and to achieve high-quality ICM.

CONCLUSIONS

In this study, we investigated the effectiveness of IM and ICM in the fabrication of 0.4-mm thin-walled LGPs with 5–10 μm v-groove microfeatures. The Taguchi method and parametric analysis were applied to study the effects of the molding parameters on the quality of the replicated microfeatures. Replication results by IM and ICM are presented. On the basis of the experimental results, we came to the following conclusions:

1. Notably, LGPs can be fabricated by both IM and ICM. The mold temperature and melt temperature were the most influential factors in IM and ICM.
2. The replication results indicate that ICM was better than IM in for the replication of v-grooved LGPs. The height of the microfeatures achieved by ICM was more accurate than that of the microfeatures achieved by IM. Additionally, LGPs produced by ICM had much less warpage than those produced by IM.
3. The compression speed and injection speed were the most important control factors in ICM for the microinjection compression molding of thin-walled LGPs. A high compression speed increased the molding quality of the LGPs. Furthermore, the experimental results indicate that a high injection speed was necessary, especially for the thin-walled microinjection compression molding process.

The authors thank Yu Jyh-Cheng for providing assistance with the measurement and Ted Knoy for his editorial assistance.

References

1. Lin, T. H.; Isayev, A. I.; Mehranpour, M. Polym Eng Sci 2008, 48, 1615.
2. Yao, D.; Kim, B. Micromech Microeng 2002, 12, 604.
3. Yao, D.; Kim, B. Injection Molding Technol 2002, 6, 11.
4. Heckele, M.; Schomburg, W. K. Micromech Microeng 2004, 14, R1.
5. Giboz, J.; Copponnex, T.; Mélé, P. Micromech Microeng 2007, 17, R96.
6. Huang, C. K. J Appl Polym Sci 2008, 107, 497.
7. Huang, M.-S.; Tai, N.-S. J Appl Polym Sci 2009, 113, 1345.
8. Xu, G.; Yu, L.; Lee, J.; Koelling, K. W. Polym Eng Sci 2005, 45, 866.
9. Sha, B.; Dimov, S.; Griffiths, C.; Packianather, M. S. J Mater Process Technol 2007, 183, 284.
10. Giboz, J.; Copponnex, T.; Mélé, P. Micromech Microeng 2009, 19, 1.
11. Yoshii, M.; Kuramoto, H.; Ochiai, Y. Polym Eng Sci 1998, 38, 1587.
12. Yao, D.; Chen, S. C.; Kim, B. Adv Polym Technol 2008, 27, 233.
13. Yokoi, H.; Han, X.; Takahashi, T.; Kim, W. K. Polym Eng Sci 2006, 46, 1140.
14. Chen, S. C.; Hu, C. H.; Chang, M.; Su, L. C. Annu Tech Conf 2006, 1246.
15. Yang, S. Y.; Ke, M. Z. Polym Eng Sci 1995, 35, 1206.
16. Chen, S. C.; Chen, Y. C.; Cheng, N. T. Int Commun Heat Mass Transfer 1998, 25, 907.
17. Wu, C. H.; Chen, W. S. Sens Actuators A 2006, 125, 367.
18. Tseng, S. C.; Liao, C. L. Int Polym Proc 2003, 2, 194.
19. Wu, C. H.; Su, Y. L. Int Commun Heat Mass Transfer 2003, 30, 215.
20. Liu, S. J.; Lin, K. Y. J Reinf Plast Compos 2005, 24, 373.
21. Shen, Y. K.; Chang, H. J.; Hung, L. H. Key Eng Mater 2007, 329, 643.
22. Huang, M.-S.; Yu, J.-C.; Lin, Y.-Z. J Appl Polym Sci, 2010, 118, 3058.